

Electrically Small Probe for Near-field Detection Applications

by

Abdulaziz Ali Alqahtani

A thesis
presented to the University of Waterloo
in fulfillment of the
thesis requirement for the degree of
Master of Applied Science
in
Electrical and Computer Engineering

Waterloo, Ontario, Canada, 2013

© Abdulaziz Ali Alqahtani 2013

I hereby declare that I am the sole author of this thesis. This is a true copy of the thesis, including any required final revisions, as accepted by my examiners.

I understand that my thesis may be made electronically available to the public.

Abstract

The microwave near-field detection technique is of interest to many researchers for characterizing materials because of its high sensitivity. It is based on sensing buried objects by producing an evanescent field. The advantage of evanescent fields is their capability to interrogate electrically small objects. In the past, near-field probes have been designed to sense magnetic materials. For dielectric materials, a near-field probe that senses the permittivity of the materials is important. This work presents a novel design of a near-field probe that generates a dominant electric field. The probe is an electrically small dipole measuring approximately 0.07λ in length operating at 216.3 MHz. The antenna is matched to a 50Ω system using two chip inductors distributed symmetrically on the dipole. The numerical and measurement results show that the proposed design is highly sensitive and capable of sensing subsurface object. The proposed design is compact, lightweight and applicable for microwave applications.

Acknowledgements

In The Name of Allah, The Most Beneficent, The Most Merciful

All praises are due to Allah for giving me the ability to write this work. All praises are due to Allah for giving me the honor of helping the humanity by contributing to enrich its knowledge.

I would like to thank my parents for providing me with the support needed in order to continually push myself to succeed. All the support they have provided me over the years was the greatest gift anyone has ever given me.

I would like to express my sincere appreciation and thanks to my advisor, Professor Omar M. Ramahi for his guidance, encouragement and continuous support through this work. The extensive knowledge, vision, and creative thinking of Prof. Ramahi have been the source of inspiration for me throughout this work.

I extend my thanks to my thesis committee members, Professor Raafat R. Mansour and Professor Mustafa Yavuz for serving in my examination committee and for their invaluable feedback.

My sincere acknowledgement to Dr. Zhao Ren for her help and guidance during this work.

I would like to thank my colleagues in the Electromagnetic group in University of Waterloo Dr. Babak Alavikia, Dr. Mohammed Boybay, Dr. Mohammed Bait Suwailam, Dr. Zhao Ren, Dr. Hussein Attia, Nael Suwan, Dr. Bing Hu, Mohammed AlShareef, Thamer Almoneef, Khawla Alzoubi, Ahmed Ashoor, Vahid Nayyeri, Abdulbaset Ali, Ali Albishi, Miguel Ruphuy, Ferhat Aydinoglu, and Humayra Naosaba for friendly discussions and inspiring conversations that always drive me to think and learn.

Special thanks to my brother Ali Albishi for his support for overcoming the difficulties during my study.

My deepest gratitude for my wife, Amal for her patience and love to accomplish my goals. My son Faisal always brings the most joyful moment at home and turns my most depressed times into colorful world.

This work was financially supported by King Saud University, Saudi Arabia.

Dedication

To my parents

To my lovely wife, *Amal*

To my precious son, *Faisal*

Table of Contents

List of Tables	viii
List of Figures	ix
List of Abbreviations	x
1 Introduction	1
1.1 Motivation	1
1.2 Thesis Objectives	2
1.3 Thesis Contribution	2
1.4 Thesis Outline	2
2 Background in Electrically Small Antennas	3
2.1 Introduction	3
2.2 Antenna Metrics	4
2.2.1 Quality Factor	4
2.2.2 Directivity	6
2.2.3 Radiation Efficiency	6
2.3 Historical Background	7
2.4 Antenna Miniaturization	10

3	Design and Fabrication of the Probe	11
3.1	Introduction	11
3.2	Near-field Probe	11
3.2.1	Background	11
3.2.2	Probe Design	13
3.2.3	Simulation Procedure	14
3.2.4	Fabrication and Measurement Procedure	15
3.2.5	Data Analysis	16
3.3	Conclusion	17
4	Results and Discussion	18
4.1	Introduction	18
4.2	Results	18
4.2.1	Simulation Results	18
4.2.2	Experimental Results	19
4.3	Discussion and Conclusion	21
5	Conclusion and Future Work	22
5.1	Conclusion	22
5.2	Future Work	22
	References	24

List of Tables

3.1 The Near-field Probe Dimensions	14
---	----

List of Figures

2.1	Chu Sphere of radius "a" [1]	4
2.2	The radiation pattern of Hertzian Dipole [1]	7
3.1	Near-field Probe Designs [2]	12
3.2	H-field Dominant Probe [2]	13
3.3	The side view of the probe structure	14
3.4	The Near-field Probe Design Using CST.	15
3.5	The Fabricated Near-field Probe	16
3.6	The Experiment Setup	16
4.1	the probe's return loss using CST	19
4.2	The electric field distribution on the probe structure	19
4.3	the probe's return loss from Experiment	20
4.4	The phase of the reflection coefficient from Experiment	20
4.5	A comparison of the magnitude of the reflection coefficient (S11) between the simulation and experiment	21

List of Abbreviations

ESA	Electrically Small Antenna
FBWV	Matched Voltage Fractional Bandwidth
FBW	3dB Fractional Bandwidth
RPF	Radiation Power Factor
TE	Transverse Electric
TM	Transverse Magnetic
VSWR	Voltage Standing Wave Ratio

Chapter 1

Introduction

1.1 Motivation

Non-invasive detection is considered a challenging area that has many applications. Some applications in this area suffer from a high error rate in the sub-surface resolution. It is important to improve the resolution of these techniques by enhancing the evanescent field produced and thus the detection sensitivity. In the literature, material characterization is one of the applications considered for sensitivity enhancement. Different techniques have been discussed for detection. Among these, researchers have given attention to microwave near-field detection techniques as an important trend for enhancing the sensitivity of detection probes. For instance, a near-field probe has been devised to sense a magnetic medium by generating a magnetic field that affects the target then to measure the probe's sensitivity by analyzing the information gained. The sensitivity of the probe can be measured by how the target responds to the evanescent wave produced by the probe. Recently, studies have discussed probes that target the magnetic medium. Interestingly, it has been discovered that the human body, for instance, contains both magnetic and dielectric materials. Accordingly, the need becomes crucial to design a new probe that detects the subsurface dielectric objects. Thus, this present study has been done to solve this problem. This work presents a novel design for a near-field probe that generates a dominant electric field.

1.2 Thesis Objectives

The work described in this thesis was motivated by the following objectives. The primary goal of this thesis is to design and fabricate a novel microwave near-field probe for near-field sub-surface detection. This probe is an electrically small dipole that operates at 216.3 MHz. It generates an E-field that dominates the near-field. The purpose is to sense the dielectric medium in a sub-surface region. The work is intended to achieve other purposes, such as

- Reviewing the theory of small antennas and the fundamental bandwidth limits
- Understanding the concept of near-field probes and their applications.
- Applying the lumped loading technique to miniaturize the antenna structure, thus leading to a shift in the resonance to lower frequency
- Validating the effectiveness of the proposed design by showing the close agreement in the results between the simulation and measurement.

1.3 Thesis Contribution

This thesis significantly contributes to the field of study by the novelty of its proposed design for a near-field detection probe. The probe works as a sensor to detect the dielectric medium beneath a surface by generating an electric field that characterizes the material's permittivity. The numerical and measurement results show that the proposed design is highly sensitive and capable of extracting the required information from the target. It is compact, lightweight and applicable for microwave applications.

1.4 Thesis Outline

The plan for this thesis is as follows; Chapter 2 reviews the theory of electrically small antennas, including their fundamental limits and some important antenna factors that are related to this work. The methodology behind designing and fabricating the proposed probe is described in Chapter 3. Chapter 4 presents the results for both the simulation and the measurement and a comparison between them with some discussion. Chapter 5 concludes the work and presents some ideas for future work.

Chapter 2

Background in Electrically Small Antennas

2.1 Introduction

One of the most important and interesting topics currently being argued in antenna and related areas is antenna miniaturization. The need for small and multifunctional antennas has been ever growing since the start of radio communication. The challenge to create smaller antennas has increased with the continuing development of wireless devices in many applications.

This chapter's review of small antenna theory is necessary to understand the challenge of antenna miniaturization. The "electrically small antennas" (ESAs) term will be used to refer to antennas with sizes much smaller than a wavelength at the frequency of operation. A suggested definition for an ESA was presented by Wheeler [3], when he described it as an antenna whose utmost size does not exceed the radianlength, i.e., $\lambda/2\pi$, where λ is the wavelength. Alternatively, a widespread ESA definition that ensures the condition is

$$ka < 0.5 \tag{2.1}$$

where k is the wave number $2\pi/\lambda$, and a is the radius of the minimum circumscribing sphere surrounding the antenna, as in Fig. 2.1. This sphere is called "Chu Sphere". It is noted that antennas confined by a Chu sphere radiate the first order spherical modes of a Hertzian dipole and have parameters such as efficiencies, bandwidths, and radiation resistances that decrease with electrical size ka [1].

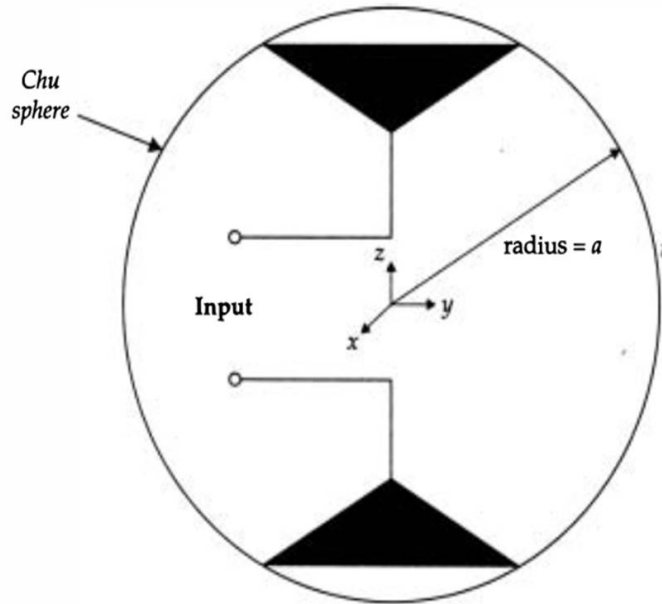


Figure 2.1: Chu Sphere of radius "a" [1]

Hansen in [4] proposed another generally agreed upon definition for an ESA that satisfies the condition $ka < 1$. In other words, it is surrounded by a sphere whose radius is one "radianlength". This sphere, called the "radiansphere" [5] sets a border between the near- and far-field radiation of a Hertzian dipole. It is observed that the higher order spherical modes are evanescent for antennas of this size [4].

2.2 Antenna Metrics

In this section, a survey of the most fundamental antenna terms will be introduced in order to lay the groundwork for augmenting the small antennas.

2.2.1 Quality Factor

In small antenna, the quality factor (Q) is considered as a substantial term that has attracted widespread attention. Harrington [6] described it as follows

$$Q = \frac{2\omega_o \max(W_E, W_M)}{P_A} \quad (2.2)$$

Where W_M and W_E are the time average stored magnetic and electric energies, and P_A is the received power by antenna. ω_o is the frequency where the small antenna is supposed to resonate either by using a lossless reactive tuning component or over self-resonance. The power radiated can be expressed in terms of the received power using the relation $P_{rad} = \eta P_A$, where η is the antenna efficiency.

A significant property of Q is that it is approximately inversely proportional to antenna's bandwidth. Q can be expressed in terms of the 3dB fractional bandwidth (FBW) in a frequently used approximation as

$$Q \approx \frac{1}{FBW} \quad \text{for } Q \gg 1 \quad (2.3)$$

Eq. 2.7 depends on the analysis of resonant circuit. As Q increases, this equation turns to be more precise. Yaghjian and Best [7] contributed a relationship between the quality factor and input impedance that is valid for resonance and anti-resonance regions as

$$\begin{aligned} Q(\omega_o) &\approx \frac{\omega_o}{2R_A(\omega_o)} \left| Z'_{in}(\omega_o) \right| \\ &= \frac{\omega_o}{2R_A(\omega_o)} \sqrt{(R'_A(\omega_o))^2 + \left(X'_A(\omega_o) + \frac{|X_A(\omega_o)|}{\omega_o} \right)^2} \end{aligned} \quad (2.4)$$

Where ω_o is the resonant frequency. $Z'_{in}(\omega_o)$ is the derivative of antenna input impedance in terms of ω_o . $R_A(\omega_o)$ and $R'_A(\omega_o)$ are the antenna input resistance and its derivative in terms of ω_o . $X_A(\omega_o)$ and $X'_A(\omega_o)$ are the antenna input reactance and its derivative in terms of ω_o .

Firstly, they determined an approximation formula of matched voltage (VSWR) fractional bandwidth (FBWV) of tuned antenna in terms of its input impedance in all frequency ranges. FBWV can be defined as the frequency range between ω_+ and ω_- with a specified VSWR.

$$FBWv(\omega_o) = \frac{\omega_+ - \omega_-}{\omega_o} \approx \frac{4\sqrt{\beta}R_A(\omega_o)}{\omega_o |Z'_0(\omega_o)|} \quad (2.5)$$

Where $Z'_o(\omega_o)$ is the derivative of feed line characteristic impedance in terms of ω_o and

$$\sqrt{\beta} = \frac{|\Gamma_{max}|^2}{1 - |\Gamma_{max}|^2} = \frac{VSWR - 1}{2\sqrt{VSWR}} \quad (2.6)$$

Eq. 2.5 still valid when β small enough (stated as $\beta \leq 1$), or similarly $FBWV(\omega_o) \ll 1$. Yaghjian and Best pointed out the benefits of using the impedances in Eq. 2.5 over conductance bandwidth and also recognized that as the impedance away from resonance, the ambiguity in the conductance bandwidth definition exists [1].

By Comparing Eqs. 2.4 and 2.5, a relationship between Q and $FBWV$ is found as

$$Q(\omega_o) \approx \frac{2\sqrt{\beta}}{FBWV(\omega_o)} \quad (2.7)$$

2.2.2 Directivity

The criterion for how directional the antenna's radiation pattern is called directivity. Small antennas are treated as short dipoles that are omnidirectional antennas with a donut-like radiation pattern, as in Fig. 2.2, with a directivity of $D = 1.5$. As in Fig 2.2, the Hertzian dipole radiates a first order of transverse magnetic (TM_{10}) or transverse electric (TE_{10}) spherical mode pattern. Harrington [6], Kwon [8, 9], and Pozar [10] determined theoretically that enclosing different configurations of electric and magnetic Hertzian dipoles may result in bidirectional and unidirectional patterns with a variety of directivity values. Because small antennas' directivity does not change when their electrical size ka is reduced, they can be categorized as superdirective antennas.

2.2.3 Radiation Efficiency

Radiation efficiency has not been discussed intensely although of its importance in small antennas. Antenna radiation efficiency factor η can be defined as the ratio of the power radiated by antenna to the input power of the antenna. In the equivalent circuit of antenna, the total loss can be represented as a combination of radiation resistance as well as loss resistance. In this case, the radiation efficiency can be formulated as follows :

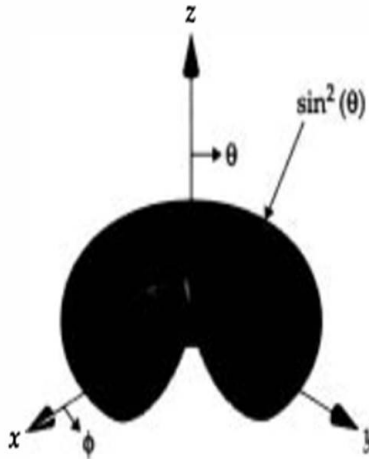


Figure 2.2: The radiation pattern of Hertzian Dipole [1]

$$\eta = \frac{R_{rad}}{R_{rad} + R_{loss}} = \frac{R_{rad}}{R_A} \quad (2.8)$$

Where R_A is the total antenna input resistance ($R_{rad} + R_{loss}$). In Eq. 2.8, the radiation loss R_{rad} decreases when the antenna size ka is reduced. However, the loss resistance controls the loss more as it has been noted; the dielectric losses within the antenna and the conduction based on frequency both are reasons mainly lead to lowering the efficiency. Harrington, lately, concluded that the losses are very notable for smaller ka values [6].

2.3 Historical Background

The first work on small antennas is attributed to Wheeler in 1947 [3]. He tried to find a relationship between the antenna size and radiation properties by applying the principle of the radiation power factor (RPF), which is a ratio of the radiated power to reactive power, to an antenna model that he derived. Simply, this model approximates the small antenna with a lumped capacitance or inductance and a radiation resistance. Through this model, he discussed the fundamental limitations of small antennas [3]. He was the first to observe that the reduction in antenna size led to a fundamental limitation on bandwidth. Wheeler

determined that the RPF was directly proportional to the physical antenna size. It can be said that the RPF was the introduction to the popular used quantity, the quality factor (Q).

The work done by Wheeler was an approximation that was only precise for small antenna sizes. This approximation was due to that not considering the radiated spherical modes when the antenna size increased. His work, nevertheless, can be recognized as the first concentrated survey of small antennas. Later on, researchers interested in this area were motivated to examine fundamental properties and limitations suggested in his work. In fact, it sparked an evolution in small antenna theory and the development of practical small antennas.

In 1948, Chu identified the minimum potential Q for an omnidirectional antenna surrounded in a Chu sphere as in Fig. 2.1 as well as the maximum gain/quality ratio (G/Q) [11]. He determines these facts by extending the spherical mode wave function to outside the mathematical sphere enclosing the antenna, i.e, expressing the radiated field as a sum of spherical modes. The Q for each mode was achieved by analyzing the equivalent lumped circuit modeled for each mode. Chu's contributions became the basis for many future researchers who overcame these restrictions although he had limited his analysis to a particular type of omnidirectional antenna. In 1981, Hansen simplified Chu's expression for calculating the minimum Q [4]. Harrington, in 1960, was the first to achieve lower minimum Q values as a result of considering that the antenna radiating both TE and TM modes [6].

As can be noticed in Chu's and Harrington's work, the equivalent circuit approximation was involved in their analysis to represent each generated mode. In 1964, Collin and Rothschild calculated the exact radiation Q [12] of an antenna radiating only TM or TE, by examining a field-based technique. As a result, the minimum Q possible is achieved surrounded in a Chu sphere. Fanta [13] later generalized their analysis to include both TE and TM modes. He determined an exact Q definition for an arbitrary TM and TE mode arrangement.

In 1996, McLean applied a different method for Q calculation that led to results consistent with Collin and Rothschild's [14]. Foltz and McLean, in 1999, reiterated Chu's analysis, using a prolate spheroidal wavefunction expansion outside a prolate spheroid, after they realized their lower Q bounds were not close to the provable values for many antennas, particularly dipoles [15]. Assuming only TM or TE modes exist, they suggested that as the spheroid becomes thinner, the Q increases proving the concept that Q is inversely proportional to the physical antenna volume.

In 2003, Thiele noted that the current distribution on an antenna strongly affects the

value of Q , after he noticed that in the earlier work, the exact lower limit of Q was far from that of actual antennas [16]. The analysis that he did in determining Q from the far-field pattern was unique since he used an expansion of the superdirective ratio concept. Thiele produced convincing results when he applied his technique to a dipole antenna with a non-uniform current distribution compared to workable dipole antennas with an identical current distribution.

Geyi in (2003–2005) started by re-examining the antenna Q and directivity restrictions, basing his work on the ideas that Chu's treatment was not sufficiently precise and that Collin's analysis involving integration was not practical for many applications [17]. Also, he presented a simpler approximation method for calculating Q , in terms of the integrations used, which were easier to work with than those of Collin and Rothschild.

Recently (2003 – 2008), comprehensive work on the theory of small antennas and their design was done by Best, Yaghjian, and their fellow workers [7, 18, 19, 20, 21, 22]. The exact and approximate expressions for Q in terms of fields, the relation between bandwidth and Q , and the impedance originated through the theoretical subjects examined by Best, Yaghjian [7]. In his work, particular self-resonant wire antennas were considered to approach the Q limits. He also discussed the impact of wire folding, wire geometry, and the volume use on Q and radiation resistance. In [20], roughly the lowest possible Q was achieved for a single radiating mode antenna when Best used his folded spherical helix antenna. The folded spherical helix design is suggestive of the spherical inductor antenna offered by Wheeler in 1958 [23].

In (2005 – 2009), Kwo and Pozar noticed a conflict between researchers in defining the TE and TM modes, the antenna gain, Q , and directionality, whilst the previous theoretical work concentrated on determining the physical restrictions on antenna Q . In [8, 9], Kwon expanded analytical work on the gain and Q associated with electric and magnetic dipoles in different structures. Then Pozar in [10] summarized Kwon's and earlier authors' findings and mentioned the diversity between the previous small antenna researchers.

In (2006 – 2009), compared to the Q values found in the past, a further confined Q was driven by Thal for some types of antennas radiating TM and TE modes and symbolized by a surface current distribution over a sphere [24]. He proposed an extra equivalent circuit that Chu did not consider in his equivalent mode circuit method. The purpose of presenting this circuit is to give a reason for the storage of energy inside the sphere. The minimum Q that Thal determined was almost equal to what Best found for spherical helix antenna [20]. In [25], Thal stated that there is dependency between the small antenna parameters such as Q , gain, and the energy inside the Chu sphere. A work by Gustafsson and other authors in (2007) derived the gain and Q formula for any small antenna with

arbitrary geometry [26].

2.4 Antenna Miniaturization

In this section, a general discussion about antenna miniaturization is presented . First, the notion of miniaturization is explained. Then, the techniques have been applied in the literature of how this concept can be achieved is mentioned.

The miniaturization idea comprises decreasing the wave's phase velocity directed by the structure of antenna in order to create resonance or coherent radiation when the antenna is electrically small. The guided-wave phase velocity v_p and the characteristic impedance Z_o are commonly expressed by

$$v_p = \frac{1}{\sqrt{LC}} = \frac{1}{\sqrt{\mu\epsilon}} \quad Z_o = G\sqrt{\frac{L}{C}} = G\sqrt{\frac{\mu}{\epsilon}} \quad (2.9)$$

where L is the series inductance per unit length, C is the shunt capacitance per unit length and G is a geometrical factor. From Eq. 2.9, the electrical delay can be well accomplished by controlling the series inductance and shunt capacitance to achieve resonance.

This concept can be achieved using one of two classes of techniques. the first approach is the material loading which means enhancing the antenna with material that satisfy $\epsilon_r > 1$ and/or $\mu_r > 1$. It considered as the most popular method for antenna designs; however, because it adds more weight to the material, it is not desirable in many applications. Also, the added material loss which affects the antenna performance is another disadvantage for this method. The reactive loading is the second approach for antenna miniaturization. The lumped elements such as series inductor and/or shunt capacitance are loaded to the antenna structure [1]. This method is preferable in most applications since its lightweight and validity for any frequency range. In this work, this method is used for the reasons mentioned.

Chapter 3

Design and Fabrication of the Probe

3.1 Introduction

In this chapter, the methodology of designing and fabricating an electrically small near-field probe at 216.3 MHz is presented. The lumped loading technique was applied to improve the small antenna performance. The main purpose of this design is to use it as a sensor in near-field detection. First, the design of the probe is reviewed. After that, the design simulation's and the measurement's procedure is explained. Finally, the way how the data analyzed is mentioned.

3.2 Near-field Probe

3.2.1 Background

Near-field probe can be defined as a tool that senses the electromagnetic properties of the materials with sub-wavelength resolution [27]. In fact, it restricts the evanescent fields to areas that are significantly smaller than the wavelength of the incident electromagnetic wave. The near-field probes' first appearance is assigned to Synge in 1928 when he discovered the first near-field microscopy. After Synge's invention, Frait and Soohoo developed probes that are sensitive to the sample properties in 1960 [28], 1962 [29] respectively. All these are aperture probes, which are created from microwave cavities with small holes. There are some typical designs of near-field probes such as waveguide with aperture, tapered waveguide with coax tip inside, open ended coaxial line, open ended coaxial line

with a small tip protruding from the inner conductor, and coaxial line with a wire loop as the tip as shown in Fig. 3.1(a,b,c,d) respectively. The near-field probes can be classified in terms of different categories such as frequency bandwidth, and geometry. For example, in terms of the frequency domain, there are broadband and resonant probes. Also, in terms of shape, there are waveguide and split ring resonator probes. The near-field probes have been utilized in near-field subsurface detection. The objective is to detect and identify the obscured objects that are beneath a buried medium by monitoring the response of the near-field probes. There are many techniques that can be used such as scanning probe microscopy, quantitative materials imaging, and multi-view tomography. In the literature, H-field dominant probes have been used to sense the magnetic buried object such as in Fig. 3.2. However, some media, such as the human body, composed of magnetic and dielectric materials and the need to use this E-field dominant probe that detects the dielectric materials becomes very important.

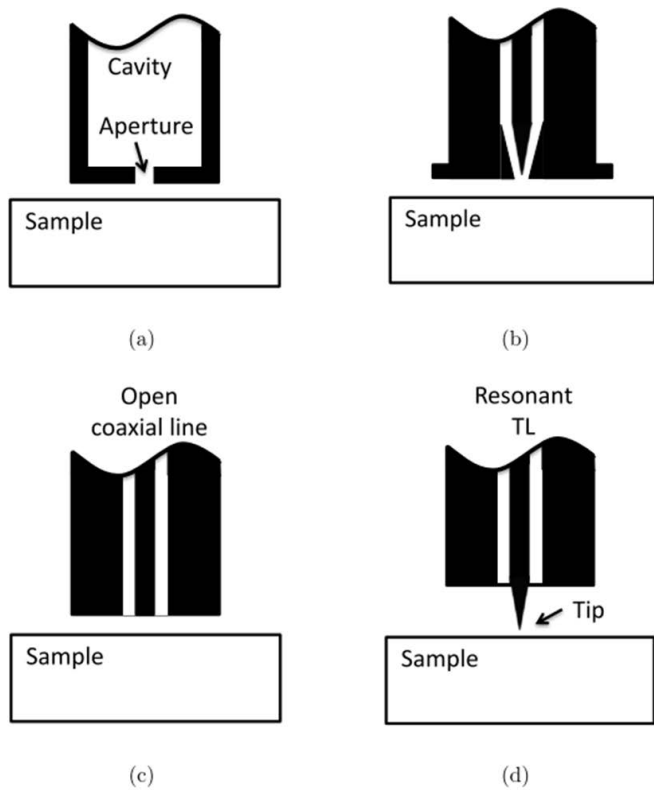


Figure 3.1: Near-field Probe Designs [2]

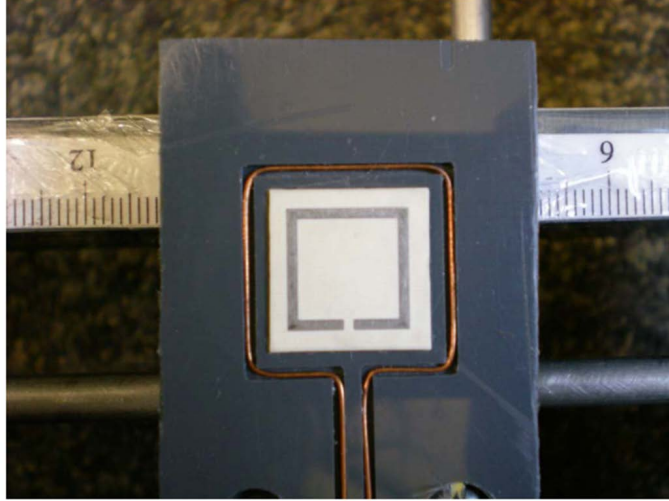


Figure 3.2: H-field Dominant Probe [2]

3.2.2 Probe Design

The proposed design is a small dipole loaded with two chip inductors. The dipole is electrically small with electrical length $ka = 0.23 < 1$, where the operational frequency is 216.3 MHz. It is designed to sense in near-field detection with very narrow bandwidth. Usually the small dipole has small radiation resistance and highly capacitive reactance. To improve the probe performance (achieve resonance), it was miniaturized by using two lumped elements, series inductors, loaded in both dipole's arms equally. The probe is fed with 50Ω coaxial cable. The plexyglas was used to balance the copper rod. The positions of the chip inductors are optimized to have the best performance. Also, the value of inductors chosen to be $300nH$. The chip inductors are used to match the input impedance and shifts the resonance to lower frequency. The inductor values were chosen to be $300nH$. The chip inductors are lossy and the internal series resistance can be calculated from the quality factor ($Q = 47$ at 250 MHz) given in the datasheet. From Eq. 3.1, the loss is 10Ω . A schematic of the structure's side view is illustrated in Fig. 3.3. In Table 3.1, the dimensions of the design are presented.

$$R = \frac{\omega L}{Q} \quad (3.1)$$

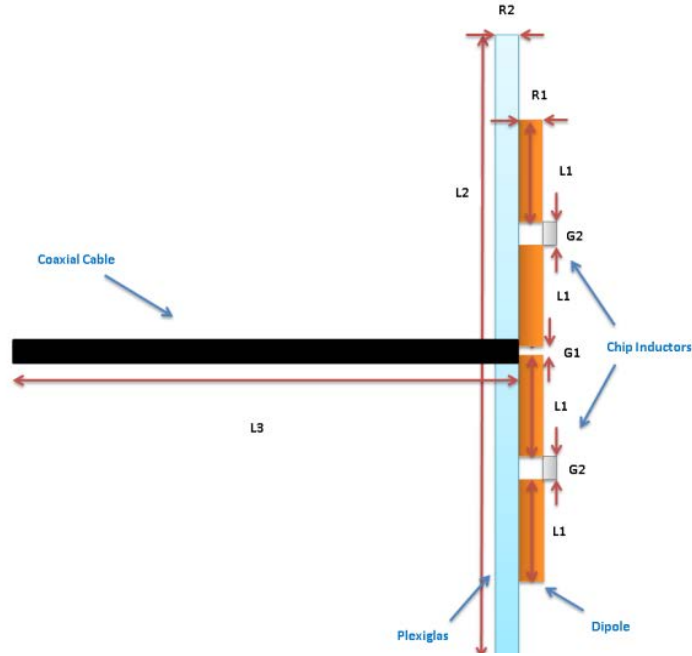


Figure 3.3: The side view of the probe structure

Parameter	Value (mm)
$L1$	24.3
$L2$	146.05
$L3$	120
$R1$	3.175
$R2$	3.175
$G1$	0.6
$G2$	1.2

Table 3.1: The Near-field Probe Dimensions

3.2.3 Simulation Procedure

In this section, the way how the probe structure was modeled and simulated is presented. First, based on the dimensions in Table 3.1, the probe was modeled and simulated using Computer Simulation Technology (CST) as shown in Fig. 3.4. The probe composed of many parts. Each part was represented with specific component. As can be seen in Fig. 3.4, symmetrical cylinders was used to represent dipole arms. Copper was used as

a material for the dipole arms. Since the chip inductor has internal loss, the lumped elements are modeled as series RLC. The values of the inductance and resistance are 300 nH, 10 Ω respectively. The design was excited with 50 Ω source which in CST equivalent to a discrete port. A plexiglas was modeled in CST as a rectangular box. In fact, high frequency structure simulator (HFSS) was used to simulate the probe. However, since the model that I used for the lumped elements is parallel RLC, the HFSS did not give good results.

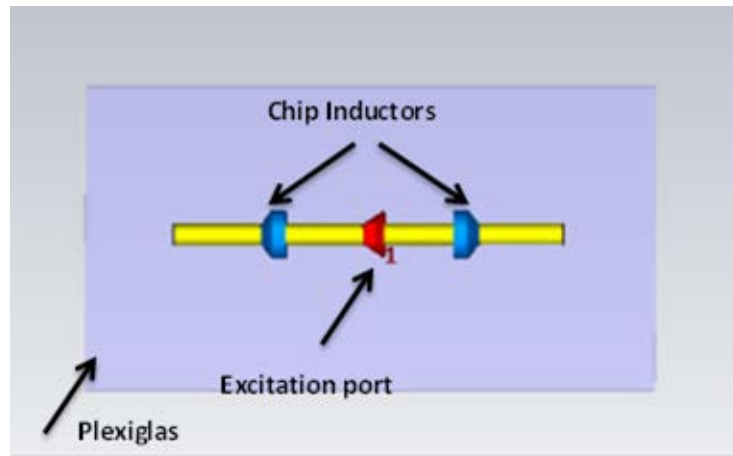


Figure 3.4: The Near-field Probe Design Using CST.

3.2.4 Fabrication and Measurement Procedure

In this section, the way how the probe fabricated and tested is presented. First, the copper rod was cut symmetrically to four pieces in the machine shop. After that, a 50 Ω coaxial cable was soldered to the dipole terminals. To balance the copper pieces in a straight line properly, they were glued on a plexiglas. The last step is soldering the chip inductors in the middle of each dipole arm. Both the soldering and the gluing processes were performed in Ramahi lab. The completed fabricated design is shown in Fig. 3.5. After the probe is ready for testing, the measurement was taken place in Mansours lab. The probe was tested using the vector network analyzer (VNA). In this measurement, first, the VNA was calibrated. Then, the probe was connected and tested through the port 1 of VNA. Fig. 3.6 shows the experiment setup in the lab.

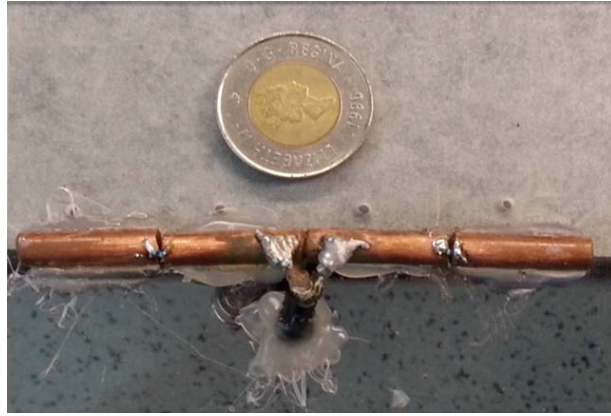


Figure 3.5: The Fabricated Near-field Probe

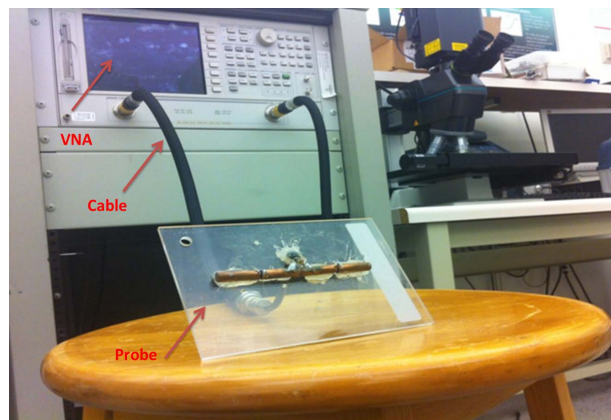


Figure 3.6: The Experiment Setup

3.2.5 Data Analysis

In this section, the way how the data was analyzed in both the simulation and measurement is described. From the CST simulator, the ASCII code of the reflection coefficient (S_{11}) response was extracted as a text file. After that, this text file was imported to MATLAB to read it as a matrix to plot the magnitude and phase of S_{11} . Similarly, in the measurement, s1p files of S_{11} magnitude and phase were extracted from VNA and were imported to MATLAB to read it.

3.3 Conclusion

The method of designing and fabricating an electrically small near-field probe at 216.3 MHz is described. First of all, a background about near-field probes that has been used in the literature as H-field dominant probes is mentioned. However, for near-field detection applications, the H-field probes do not accurately extract the body information. As a result, the proposed E-field probe is designed in this work to tackle this problem. The procedure how the near-field probe is simulated and fabricated was explained in detail.

Chapter 4

Results and Discussion

4.1 Introduction

In order to validate the principle of using the probe as a sensor for near-field detection, the proposed design was simulated using the CST and tested in the lab. The proposed near-field probe is considered as electrically small, i.e., its size is much smaller than a wavelength at the operational frequency where this condition $ka < 1$ is satisfied. Typically, electrically small antennas have narrow bandwidth, in other words, high quality factor. For this reason, this design is suitable for detection applications in near-field regime because of its high sensitivity. In this chapter, both the simulation and experimental results and some discussion are presented.

4.2 Results

4.2.1 Simulation Results

Fig. 4.1 shows the magnitude of the reflection coefficient (return loss) for a 50Ω source using CST simulator. The probe resonates around 253 MHz and matched to 50Ω with -17.39 dB. Typically, a small dipole is a source of TM mode evanescent fields. From Fig. 4.2, it is shown that the probe generates electric field which is concentrated at the excitation location of the dipoles. The voltage standing wave ratio (VSWR) is 1.312:1 and the fractional matched VSWR bandwidth (FBWV) at 10 dB ≈ 0.0118 resulted in $Q_{10dB} \approx 23.08$ using Eq. 2.7

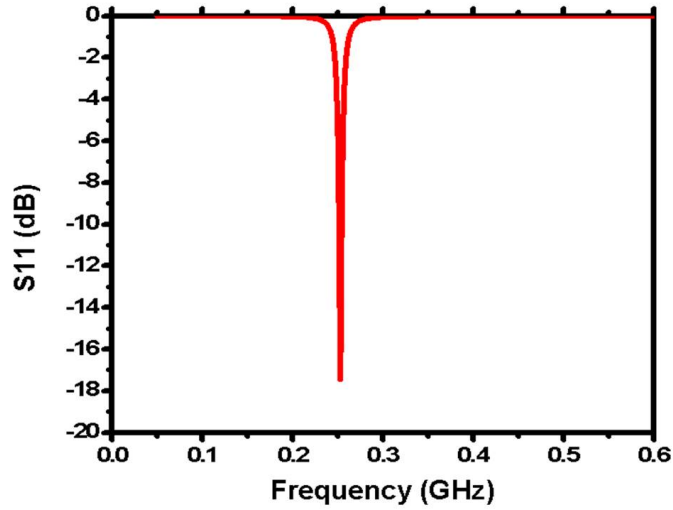


Figure 4.1: the probe's return loss using CST

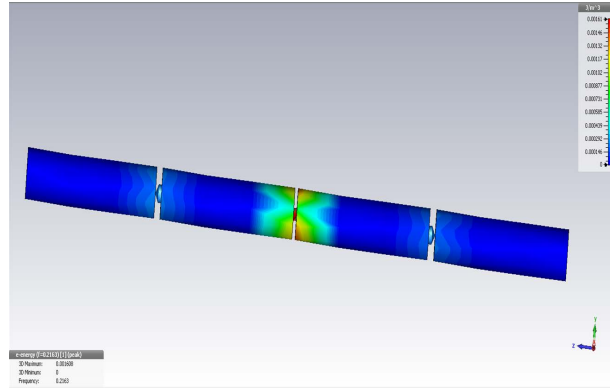


Figure 4.2: The electric field distribution on the probe structure

4.2.2 Experimental Results

To validate the sensitivity of the proposed design, the probe was fabricated and tested in the lab using the Vector Network Analyzer (VNA). The amplitude and phase of the reflection coefficient as a function of frequency are measured as in Figs. 4.3 and 4.4. Fig. 4.3 shows The near-field probe return loss from the measurement . As can be seen, the probe resonate at 216.3 MHz with -11.73 dB. The phase of the reflection coefficient was plotted as can be shown in Fig. 4.4. Fig. 4.5 shows a comparison of the magnitude

of the reflection coefficient (S_{11}) between the simulation and experiment results. As can be seen, a good agreement with a slight frequency shift of 0.04 GHz was achieved.

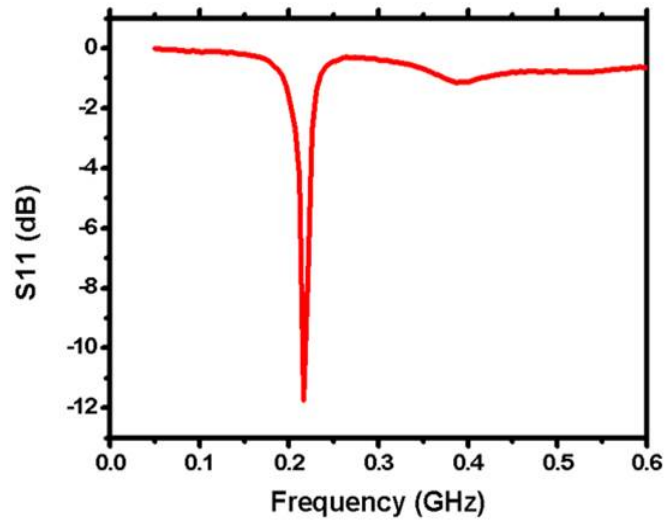


Figure 4.3: the probe's return loss from Experiment

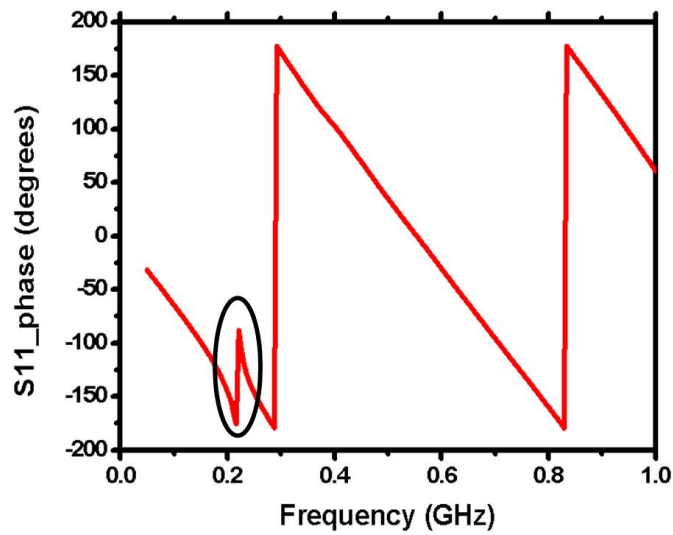


Figure 4.4: The phase of the reflection coefficient from Experiment

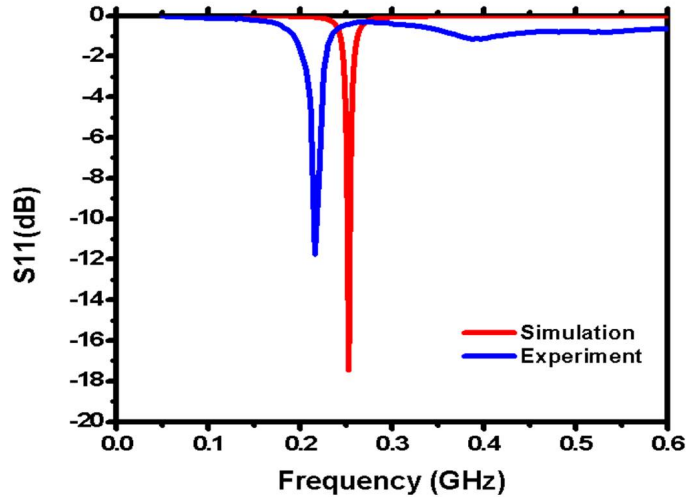


Figure 4.5: A comparison of the magnitude of the reflection coefficient (S_{11}) between the simulation and experiment

4.3 Discussion and Conclusion

In the near-field, this probe generates a near field distribution dominated by electric field. However, in far-field, it is not radiating much power because of the control of loss resistance which includes the conduction loss of the copper as well as the inductor's losses. The probe is very sensitive in near-field since of the high quality factor. An interesting observation is that at the resonant frequency, there is discontinuity in the phase response which indicates phase shift exists. In this chapter, the results of designing electrically small near-field probe and discussion about the results are illustrated. The amplitude and the phase of the reflection coefficient as a function of frequency are presented and compared in Fig. 4.5. In fact, the experimental and numerical results show very similar results. Moreover, a good discussion about the results is mentioned.

Chapter 5

Conclusion and Future Work

5.1 Conclusion

This thesis presents a novel electrically small probe for near-field detection. The probe was modeled and simulated using Microwave CST software. Then, it was fabricated and tested in the lab with the same dimensions. The technique that is used to miniaturize the antenna is the lumped loading, whereby two chip inductors distributed equally on both arms.

The simulation and measurement results achieved are promising. The probe resonates at 216.3 MHz. It is noticed that the magnitude of the reflection coefficient has a very narrow bandwidth, which means that the probe is highly sensitive. From the measurement results, at the resonance frequency, there is discontinuity in the phase of the reflection coefficient, indicating that the probe is affected by the changing of the near-field distribution in close proximity. A good agreement exists between the simulation and measurement results where the shift in the frequency is 0.04 GHz. The design appears to be very sensitive to dielectric media since it generates an E-field that dominates and characterizes subsurface materials.

5.2 Future Work

In future work, a more suitable and practical probe that is practical for near-field detection applications is planned to design. Also, some experiments with dielectric media is planned to conduct. Moreover, characterizing the materials using near-field theory and numerical

techniques, such as Fourier transform and perturbation theory, is pursued in the future in order to analyze the evanescent field of the target.

References

- [1] J. Volakis, C. Chen, and K. Fujimoto, *Small antennas: miniaturization techniques & applications*. 2010.
- [2] Z. Ren, *Microwave near-field probes to detect electrically small particles*. PhD thesis, University of Waterloo, 2013.
- [3] H. Wheeler, “Fundamental Limitations of Small Antennas,” *Proceedings of the IRE*, vol. 35, pp. 1479–1484, Dec. 1947.
- [4] R. Hansen, “Fundamental limitations in antennas,” *Proceedings of the IEEE*, vol. 69, no. 2, pp. 170–182, 1981.
- [5] T. Simpson and J. Cahill, “The Electrically Small Elliptical Loop with an Oblate Spheroidal Core,” *IEEE Antennas and Propagation Magazine*, vol. 49, pp. 83–92, Oct. 2007.
- [6] R. Harrington, “Effect of antenna size on gain, bandwidth, and efficiency,” *Journal of Research of the National Bureau of . . .*, vol. 64, no. 1, p. 7119, 1960.
- [7] A. Yaghjian and S. Best, “Impedance, bandwidth, and Q of antennas,” *IEEE Transactions on Antennas and Propagation*, vol. 53, pp. 1298–1324, Apr. 2005.
- [8] Do-Hoon Kwon, “On the radiation Q and the gain of crossed electric and magnetic dipole moments,” *IEEE Transactions on Antennas and Propagation*, vol. 53, pp. 1681–1687, May 2005.
- [9] D.-H. Kwon, “Radiation Q and Gain of TM and TE Sources in Phase-Delayed Rotated Configurations,” *IEEE Transactions on Antennas and Propagation*, vol. 56, pp. 2783–2786, Aug. 2008.

- [10] D. Pozar, “New results for minimum Q, maximum gain, and polarization properties of electrically small arbitrary antennas,” *Antennas and Propagation, 2009. EuCAP 2009. . . .*, pp. 1993–1996, 2009.
- [11] L. J. Chu, “Physical Limitations of Omni-Directional Antennas,” *Journal of Applied Physics*, vol. 19, no. 12, p. 1163, 1948.
- [12] R. Collin and S. Rothschild, “Evaluation of antenna Q,” *IEEE Transactions on Antennas and Propagation*, vol. 12, pp. 23–27, Jan. 1964.
- [13] R. Fante, “Quality factor of general ideal antennas,” *IEEE Transactions on Antennas and Propagation*, vol. 17, pp. 151–155, Mar. 1969.
- [14] J. S. McLean, “A re-examination of the fundamental limits on the radiation Q of electrically small antennas,” *IEEE Transactions on Antennas and Propagation*, vol. 44, p. 672, May 1996.
- [15] H. Foltz and J. McLean, “Limits on the radiation Q of electrically small antennas restricted to oblong bounding regions,” in *IEEE Antennas and Propagation Society International Symposium. 1999 Digest. Held in conjunction with: USNC/URSI National Radio Science Meeting (Cat. No.99CH37010)*, vol. 4, pp. 2702–2705, IEEE, 1999.
- [16] G. Thiele, P. Detweiler, and R. Penno, “On the lower bound of the radiation Q for electrically small antennas,” *IEEE Transactions on Antennas and Propagation*, vol. 51, pp. 1263–1269, June 2003.
- [17] W. Geyi, “Physical limitations of antenna,” *IEEE Transactions on Antennas and Propagation*, vol. 51, pp. 2116–2123, Aug. 2003.
- [18] S. Best, “The performance properties of electrically small resonant multiple-arm folded wire antennas,” *IEEE Antennas and Propagation Magazine*, vol. 47, pp. 13–27, Aug. 2005.
- [19] S. Best, “Bandwidth and the lower bound on Q for small wideband antennas,” in *2006 IEEE Antennas and Propagation Society International Symposium*, pp. 647–650, IEEE, 2006.
- [20] S. Best, “The radiation properties of electrically small folded spherical helix antennas,” *Antennas and Propagation, IEEE Transactions on*, vol. 52, no. 4, pp. 953–960, 2004.

- [21] S. Best, “Low Q electrically small linear and elliptical polarized spherical dipole antennas,” *Antennas and Propagation, IEEE Transactions on*, vol. 53, no. 3, pp. 1047–1053, 2005.
- [22] S. Best and J. Morrow, “On the significance of current vector alignment in establishing the resonant frequency of small space-filling wire antennas,” *IEEE Antennas and Wireless Propagation Letters*, vol. 2, no. 1, pp. 201–204, 2003.
- [23] H. Wheeler, “The Spherical Coil as an Inductor, Shield, or Antenna,” *Proceedings of the IRE*, vol. 46, pp. 1595–1602, Sept. 1958.
- [24] H. Thal, “New Radiation Limits for Spherical Wire Antennas,” *IEEE Transactions on Antennas and Propagation*, vol. 54, pp. 2757–2763, Oct. 2006.
- [25] H. Thal, “Gain and Q Bounds for Coupled TM-TE Modes,” *IEEE Transactions on Antennas and Propagation*, vol. 57, pp. 1879–1885, July 2009.
- [26] M. Gustafsson, C. Sohl, and G. Kristensson, “Physical limitations on antennas of arbitrary shape,” *Proceedings of the Royal Society A: Mathematical, Physical and Engineering Sciences*, vol. 463, pp. 2589–2607, Oct. 2007.
- [27] S. Anlage, V. Talanov, and A. Schwartz, “Principles of near-field microwave microscopy,” *Scanning probe microscopy*, 2007.
- [28] Z. Frait, V. Kamberský, Z. MÁlek, and M. Ondris, “Local variations of uniaxial anisotropy in thin films,” *Czechoslovak Journal of Physics*, vol. 10, pp. 616–617, Aug. 1960.
- [29] R. F. Soohoo, “A Microwave Magnetic Microscope,” *Journal of Applied Physics*, vol. 33, p. 1276, Mar. 1962.